An Analog Front-End for an ISFET-Based Sensor Using Off-The-Shelf Components

Ronaldo Martins da Ponte
Department of Electrical Engineering
UFSC - Federal University of Santa Catarina
Florianópolis, Brazil
Email: ronaldo.m.ponte@ieee.org

Fernando Rangel de Sousa
Department of Electrical Engineering
UFSC - Federal University of Santa Catarina
Florianópolis, Brazil
Email: rangel@ieee.org

***Abstract*—In this paper, an analog front-end (AFE) to condition ISFET-based sensors is presented. This is accomplished by a pH-controlled ring oscillator (pHCO) able to produce a pulse frequency-modulated signal proportional to the pH of the testing solution. A sensor's electrical characterization was carried out to supply electrical parameters for its Verilog-based model. The conditioning technique was demonstrated from electrochemical results obtained by the discrete-circuit implementation. Measurements using standard buffer solutions with pH value of 4, 7 and 10 found 0.9985 of R^2 coefficient and 2% of linearity error - denoting its goodness of fit with the linear model. Moreover, the circuit topology circumvents the body effect problems, suppress the use of OP-AMPs or ADCs, and allows for future monolithic integration.**

I. Introduction

In a measurement system, sensors are used to convert a physical input variable on a corresponding electrical output. As the electrical signal on its output is usually weak, an analog front-end (AFE) is required to condition the signal before convey it to post-processing blocks. Therefore, the AFE plays an important role in the instrumentation system as it shall be designed to detect weak signals while ensuring information integrity to be subsequently shown.

Moreover, the AFE design is further strongly dependent on the sensor features. One key advantage to select a suitable sensor element relies on assuring its compatibility with semiconductor fabrication methods, giving scope for monolithic integration of the sensors and intending to support the design of low-power, small-sized and fast response time systems. Between this and that, we present in this work an AFE for an ISFET-based sensor using off-the-shelf components.

The ISFET, Ion-sensitive Field-effect Transistor, is a chemically sensitive FET conceived in 1970 by Bergveld [1] that can sense pH levels arising in the test solution since its insulating membrane is sensitive to hydrogen ions. Thus, any change in the pH level charges a potential profile across the solution causing a modulation in the ISFET threshold voltage.

Despite the progress on novel input stages, much of the literature has focused on only two AFE topologies for ISFET: the source-drain followers [2] and the differential pair schemes [3]. The first one demerits the ISFET's transistor-like behaviour by forcing a single operating point on it at constant drain-to-source voltage and constant drain current to track changes in the threshold voltage caused by a pH level flutuation. In addition, this configuration suffers from body bias, which undertakes the readout sensitivity of the circuit. On the other hand, the differential pair provides benefits by virtue of its common-mode rejection, although its realization in practice is challenging due to differences between the ISFET threshold voltage and its MOSFET counterpart. Both configurations output a voltage proportional to the pH of testing solution. A final and equally important point is that AFE circuits are generally used to hold the information upon the electrical signal amplitude, therefore, requiring an analog-to-digital converter (ADC) which accounts for further circuit design, silicon area and power consumption.

In this work, we designed an AFE that converts the pH information automatically to digital domain via pulse-frequency modulation (PFM), therefore, overcoming the ADCs use in the system. This was solved by a pH-controlled ring oscillator (pHCO) whose current is controlled by the pH level arisen upon the sensor surface, so that the output signal becomes digitally-represented by the pH level. The conditioning technique was confirmed from the results obtained via a circuit implementation using off-the-shelf components. The ISFET-based sensor was fabricated by another research group sited in Campinas city, Brazil.

II. ISFET operation

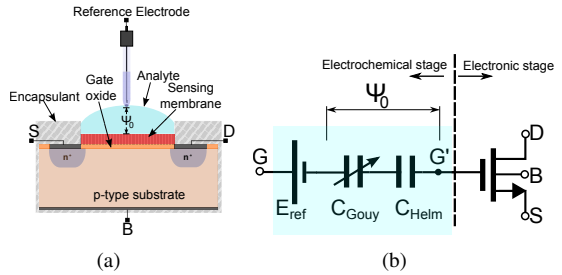

(a) (b)

Fig. 1: (a) ISFET device; (b) Behavioral ISFET model

ISFETs are ion-selective electrochemical sensors being derived from a simple MOSFET (Figure 1(a)), in which its gate terminal is coated with a material used to sense ions concentration (usually H^+).

The principle of ISFET operation is related to chemical reactions happening in the oxide-electrolyte interface. Such mechanisms are best described by the site-binding and electrical double layer theory [4], where H^+ ions presented in the analyte are adsorbed by the sites presented in the hydrated oxide surface producing a potential profile (Ψ_0) across Gouy-Chapman and Helmholtz capacitances (Figure 1(b)). The potential profile is proportional to the pH as stated in the general expression of the ISFET pH sensitivity:

$$\frac{\partial \Psi_0}{\partial pH} = -2.3\frac{kT}{q}\alpha \tag{1}$$

where kT/q is the thermal voltage and α a dimensionless parameter ranging between 0 and 1. The parameter Ψ_0 modifies the flat-band voltage of the device, which in turn is directly related to its threshold voltage. Accordingly, pH changes in the analyte produces a change in the threshold voltage as per Equation (2):

$$V_{T0_{ISFET}} = E_{ref} + \Delta\varphi^{lj} - \Psi_0 + \chi_{sol} - \frac{\phi_{Si}}{q} - \left(\frac{Q_{ss} + Q_{ox} + Q_B}{C'_{ox}}\right) + 2\phi_F + \gamma\left(\sqrt{2\phi_F + V_{SB}} - \sqrt{2\phi_F}\right) \tag{2}$$

where E_{ref} is the reference electrode potential relative to vacuum, $\Delta\varphi^{lj}$ the potential drop between the reference electrode and the analyte, Ψ_0 the surface potential resulted from the chemical reaction, χ_{sol} the surface dipole potential of the analyte, ϕ_{Si} the silicon workfunction, q the electrical charge, Q_{ss} the surface state density at the silicon surface, Q_{ox} the fixed oxide charge, C'_{ox} the oxide capacitance per unit area, Q_B the depletion charge, ϕ_F the Fermi-potential, γ the body-effect and V_{SB} the source-to-bulk voltage.

A. ISFET behaviour model

Considering these operation mechanisms, and referring to the work presented in [5], a Verilog-based ISFET model was designed to be applied as part of the circuit simulation and, hence, obtaining results reliable. As proposed in [5], chemical and electronic stages of the ISFET model were fully decoupled - yet still preserving the relationship between them. An experimental characterization of the ISFET testing devices was performed to extract the process parameters to be supplied into the electronic stage of the Verilog-based ISFET model.

1) Sensor Characterization: The parameter extraction used in the testing devices was based on the g_m/I_D methodology. The setup measurement is shown in Figure 2. In this setup, the gate voltage V_G was swept from 0 V to 2.0 V on the SMU-1 (Source-Measurement Unit) under a fixed drain voltage V_D forced at half of the thermal voltage, i.e. 13 mV, on the SMU-2. The circuit's reference voltage (ground) was forced on the SMU-3.

Next in order, the g_m/I_D device characteristic curve was generated and used to find the equilibrium threshold voltage (V_{TO}) and the specific current of the model (I_S). The curve in Figure 3 depicts the point at which g_m/I_D drops to 53 % of its peak value. The gate voltage measured at this point corresponds to V_{TO}, and the corresponding drain current is aproximately the specific current I_S. From this current, K_p parameter was found, since:

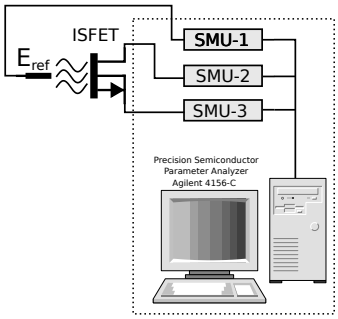

Fig. 2: Setup measurement used for the sensor characterization.

$$K_P = \mu C'_{ox} = \frac{I_S}{\frac{W}{L} n \frac{\phi_t^2}{2}} \tag{3}$$

where ϕ_t, in Equation (3), refers to the thermal voltage.

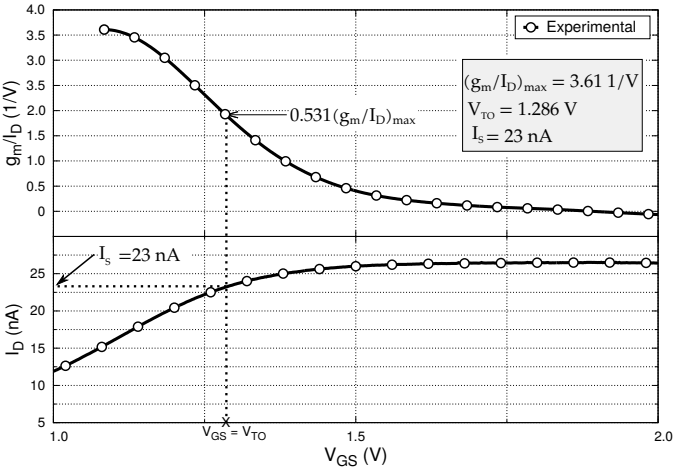

Fig. 3: Parameters obtained: equilibrium threshold voltage (V_{T0}), specific current (I_S) and the maximum transconductance-to-current ratio $(g_m/I_D)_{max}$.

The results found were then used in the Verilog-A electronic stage as reported in Table I.

Parameters	Value
V_{TO}	1.286 V
I_S	23 nA
$(g_m/I_D)_{max.}$	3.61 1/V
K_p	1 $\mu A/V^2$
W/L	2850 μm / 50 μm

TABLE I: Sensor characterization results

With both chemical and electronic stages duly supplied, we have plotted the IxV simulation characteristic curve and fitted it with the experimental results found. That being necessary

because of shifts arisen from imbalances over the fabrication process. In our experiment, higher contact impedances at source-and-drain diffusion regions were found, as reproduced in Figure 4 by the slightly S-shaped curve around the very beginning of linear region over the experimental results.

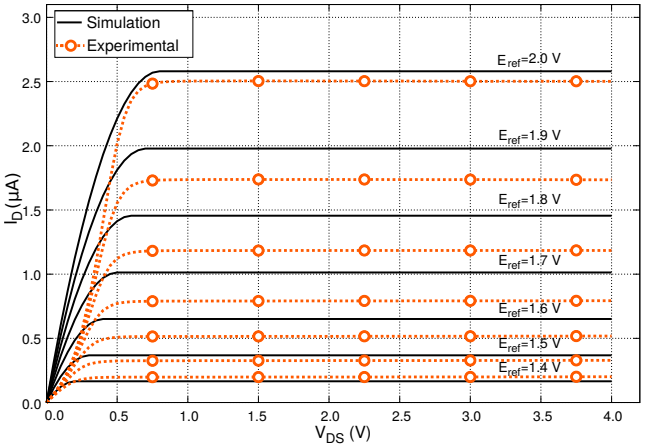

Fig. 4: Fitting between simulation and experimental curves of the ISFET-based sensor testing device.

B. Sensor Fabrication

The ISFET devices used herein were designed and fabricated at the Centro de Componentes Semicondutores (CCS), Unicamp, Brazil. The first batch furnished was organized in an array comprising 3x19 sensing elements with 50 μm/50 μm of aspect ratio each using a TiOx (Titanium dioxide) film.

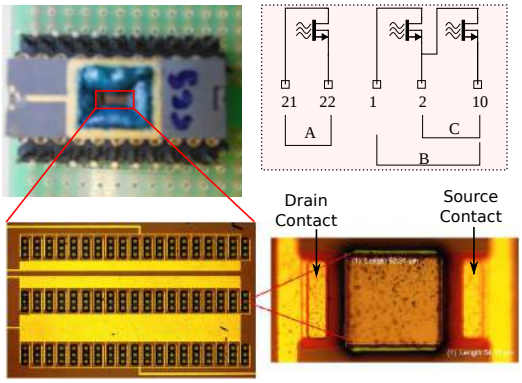

Fig. 5: Top left: photo of the encapsulated chip furnished by the CCS. Lower left: ISFETs matrix (3x19) from the view of an optical microscope. Bottom right: Detail of the sensor array elements. Top right: Welding diagram of the chip

III. Review of ISFET interface circuits

This section overviews the main topologies employed for ISFET conditioning.

A. Source-drain followers

One of well-known topologies are those whose the ISFET electrical signal is sensed from source-drain follower schemes [2]. The main idea behind these structures is to bias the ISFET with constant drain-to-source voltage and drain current (CVCC), while maintaining reference electrode at a constant potential (usually ground). The CVCC biasing technique is widely reported as the best method to know pH value, once the buffered ISFET source voltage measures only the threshold voltage changes due to pH fluctuations, from gate-to-source voltage. Thus, ISFET threshold voltage is not only affected by Ψ_0, but aditionally with the body effect, that will degradate the conditioning circuit performance because of the ISFET sensitivity reduction and the introduction of second-order temperature effects, as stated in equations 1 and 2.

B. Topologies with feedback

To circumvent the body effect drawbacks, the work presented in [6] reports an interface circuit to equalize the ISFET current and the current of constant current source by means of direct feedback to reference electrode or indirect feedback to current source. In the direct feedback structure, the output is sensed in the reference electrode. The scheme is simple, but it may suffer from stability issue due to the two high impedance nodes in the feedback structures as already pointed in [7], which leads to some op-amp design constraints related to improve phase-margin and minimize noise coupling.

C. Differential pair

Some others approaches employ differential schemes such as ISFET/MOSFET, ISFET/REFET and ISFET/ISFET differential schemes to perform temperature compensations via common-mode rejection. ISFET/MOSFET pair is difficult to implement due to the explicit intrisic differences in threshold voltage pair, resulting in a bias difference and mismatch [1]. By this reason, ISFET/REFET pair is more used since when connected in a differential mode produces a strictly pH sensitive output. Unfortunately, a stable attachment usually comes with a polymer with a given resistivity accountable for changing the electrical relaxation time, which is a measure for the time needed to redistribute the charge and establish potential profiles in the polymer after application of an electrical field [1].

D. Digital readouts for AFE minimization

Exploring the digital domain, [8] have proposed a readout scheme with minimum analog components to minimize parasitic and noise effects in large-scale chemical sensing arrays. For each array pixel, a pair of complementary ISFETs shares the same floating gate in an inverter configuration whose output is a chemically-controlled pulse-width modulated signal. In [9], an ISFET averaging array employing global negative current feedback is used to modulate VCO frequency of a first order sigma-delta modulator.

IV. The pHCO description

The AFE topology presented in this work, and henceforth named as pHCO, obtains the pH information via pulse-frequency modulation of the signal, as described in Figure 6.

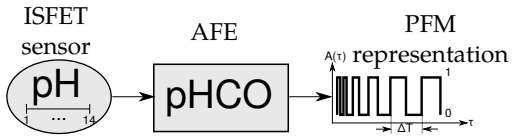

Fig. 6: Conceptual design of the ISFET conditioning system using PFM.

In this scheme, the sensor's electrically-weak signal becomes digitally-represented by virtue of the AFE so that the pulse frequency is proportional to the pH level of the testing solution. Therefore, we have eliminated the power-consuming ADC from the instrumentation system, thus, solving for system complexity, power constraints and further block design. In addition, signal-amplitude saturation issues affecting some topologies - because of the OP-AMPs usage in feedback mode - are no more a prominent drawback. Moreover, in this topology, the source and bulk ISFET terminals are shorted eliminating, thus, the body effect constraints and the introduction of second-order temperature effects.

A. Dynamic analysis of the pHCO

The pHCO circuit comprises an N-stage single-ended ring oscillator in which the delay stage has a CMOS inverter on a push-pull configuration. The number N of stages to be considered shall affect the expected oscillation frequency as per Equation (4), [10]:

$$f_o = \frac{1}{N \cdot Tp} \tag{4}$$

where T_p is the propagation time of the inverter cell.

All nMOS sources included in the ring oscillator are connected to the ISFET drain contact, which, successively, is diode-connected. Therefore, the ISFET operation can be described as the current source controlled by the potential V_{chem} as reproduced in Figure 7.

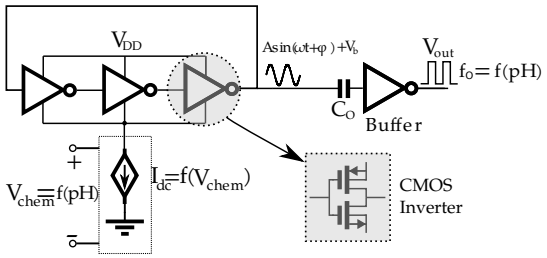

Fig. 7: Conceptual representation of the pHCO circuit

As long as inverters operate as linear amplifiers, the ring oscillator outputs a sinusoidal signal consisting of A amplitude, ω frequency and V_b DC level - all pH-dependent. Since the DC level is removed by C_o capacitor and, afterwards, the buffer gain saturates the signal amplitude, V_{out} output produces digital pulses whose pH information is encoded only in frequency domain.

B. Static analysis of the pHCO

Figure 8(a) reproduces, in short, the self-biasing circuit used to establish the ISFET DC operating point. In this figure, the ring oscillator is represented by the active load Z_L, while V_{chem} denotes for a pH-dependent potential arising upon ISFET surface.

As follows, a change in pH of the testing solution shall reflect a change in potential V_{chem} - drawing the current I_D. Passage of I_D through Z_L produces the potential V_G, which yields the error voltage $V_G^{'}$ when compared to the setpoint V_{chem}. As a result, the potential $V_G^{'}$ built is accountable for establishing the operating point of I_D. Along these lines, this self-biasing circuit is realized via serie-series feedback, as better depicted in Figure 8(b).

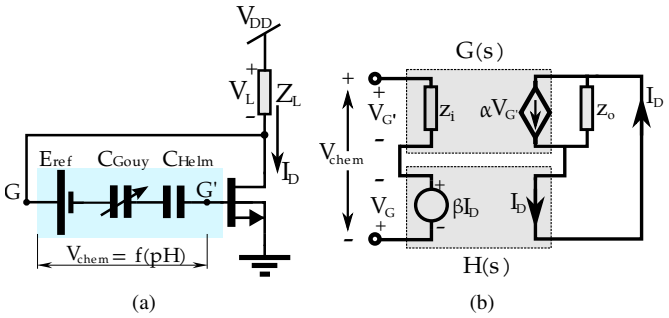

Fig. 8: Static analysis of the pHCO: (a) Simplified circuit representation. (b) Diagram adressing local negative feedback.

Moreover, a circuit analysis verifies that voltage V_L changes linearly with pH. Assuming that AFE is designed to force ISFET operation in weak-inversion mode, I_D current can be expressed as:

$$I_D = I_0 e^{\frac{V_G - \gamma - \alpha S_N pH - V_{TH_{MOSFET}}}{n\phi_t}} \tag{5}$$

As $V_G = V_{DD} - V_L$, Equation (5) can be rewritten as:

$$I_D = I_0 e^{\frac{V_{DD} - V_L - \gamma - \alpha S_N pH - V_{TH_{MOSFET}}}{n\phi_t}} \tag{6}$$

Solving for V_L, and supported by Equation (6), one obtains:

$$V_L = V_{DD} - n\phi_t \ln\left(\frac{I_D}{I_O}\right) - \gamma - \alpha S_N pH - V_{TH_{MOSFET}} \tag{7}$$

To simplify, the pH-independent terms in Equation (7) were grouped in K_V constant, as folowing by Equation (8).

$$V_L = K_V - n\phi_t \ln\left(\frac{I_D}{I_O}\right) - \alpha S_N pH \tag{8}$$

As Equation (8) is only numerically-solved, the linear dependence between V_L and pH can be assured via simulation - using both BSIM3v3 MOSFET model and Verilog-based ISFET model. The results are shown in Figure 10.

From the given figure, one can observe both simulation curve and its ideal linear trendline. A measurement of the goodness of fit with the linear model can be ensured by the

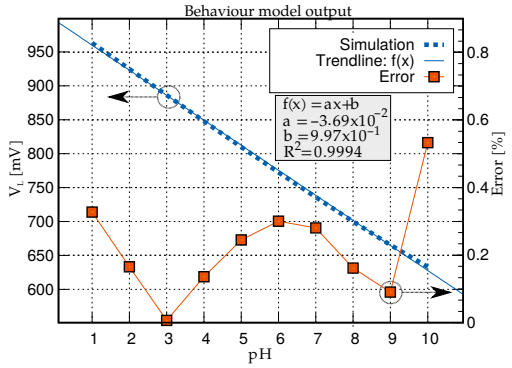

Fig. 10: Linear relation between V_L and pH.

coefficient of determination (R^2). Accordingly, a 0.9994 of R^2 coefficient was found supporting the linear dependence between V_L and pH. As a result, a linear relationship between pH and f_o oscillation frequency is found since f_o, in steady state, is inversely proportional to the delay time t_p of CMOS inverter. As t_p is the time difference between input and output threshold voltages, a V_L change produces an inversely proportional change to t_p. Wherefore, f_o holds a linear dependence with the pH of testing solution and pH information can be recovered it, afterwards, via post-processing circuits. One can further notice, from Figure 10, 0.5 % of error found at pH 10 between simulation and trendline curves and linear regression terms found.

V. Implementation of the Proposed Circuit and Results

In order to verify the electrical performance of the proposed circuit, electrochemical measurements were carried out. The main purpose is to test its functionality properly, evaluating the output waveforms and linearity in a realistic electrochemical enviroment. Thus, three standard buffers solutions with pH value of 4, 7 and 10 were applied on the sensor for pH measurement. The ISFET sensor was cleaned using DI water 18 MΩ-cm every time before it was inserted into a new buffer solution with different pH value. The temperature had been controlled at 23 °C to avoid interference in the measurements and a calomel reference electrode used to preserve the long-term stability of the TiOx sensitive film.

The circuit was built on a breadboard using off-the-shelf electronic components. The CD4007 was used for the CMOS inverter and, then, a five-stage CMOS ring oscillator was implemented using a ± 2.0 V of supply voltage. The waveform results obtained from the oscilloscope are presented in Figure 9.

One can observe, from this figure, digitally-represented waveforms and its frequency dependence with the pH of the testing solution - which suggests the functionality of the conditioning technique. The output frequency obtained for the pH value of 4, 7 and 10 was, respectivally, 93.5 kHz, 65.5 kHz and 41 kHz which corresponds to 0.9985 of R^2 coefficient - denoting, thus, its goodness-of-fit consistency with the linear model. Further, compared with the linear treandline, only a 2 % of uppermost linearity error was found at the pH value of 7. Moreover, the results indicate a 28 kHz of span over the pH 4 to 7 and a 25 kHz of span over the pH 7 to 10 denoting, in average, a rough responsitivity of 9 kHz/pH which corresponds to three times the result presented in the work [9] (3 kHz/pH) adressing, hence, the competitive edge of the conditioning technique presented in this work.

In order to get a better evaluation of its performance, the so-called source-drain follower conditioning circuit (Figure 11) was built on a breadboard using off-the-shelf components for measurement results confrontation. The LM-324 was used as the OP-AMP, the BF-245 and the J176 as the n-type and p-type JFETs, and the C547B and the C557B as the NPN and PNP BJT devices, respectively.

The source-drain follower conditioning principle resides in the fact that V_{DS}, caused by I_{BIAS1} passing through R_{DS}, is copied to ISFET's source-and-drain terminals by the voltage followers. As the ISFET drain current is tied by I_{BIAS2}, and V_{DS} is kept constant, a pH change is reflected to the ISFET source terminal and fed it back to the drain terminal by the voltage follower jointly with R_{DS}. Therefore, the pH of testing solution may be measured at the buffered terminal V_{out} as per Equation (9):

$$V_{out} = V_{REF} - V_{th_I} - \frac{I_{BIAS2}}{\beta \cdot I_{BIAS1} \cdot R_{DS}} - \frac{I_{BIAS1} \cdot R_{DS}}{2} \tag{9}$$

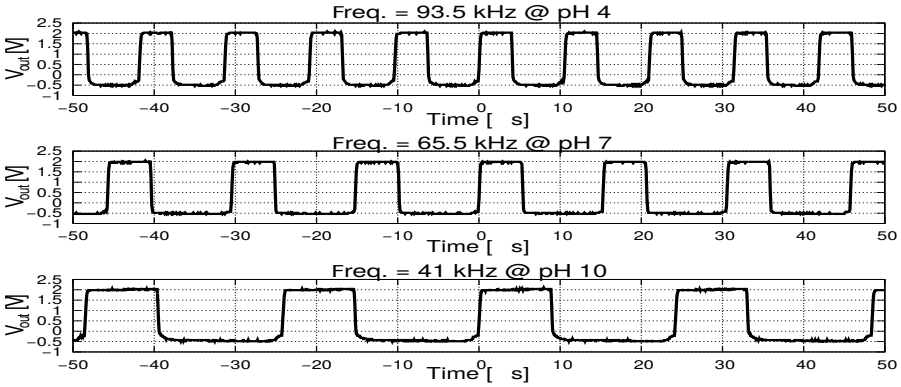

Fig. 9: The pHCO corresponding waveforms using buffers pH 4, 7 and 10.

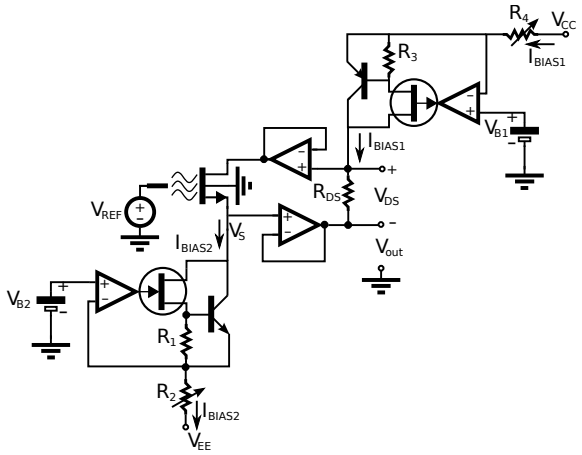

Fig. 11: Source-Drain Follower conditioning circuit

where V_{th_I} denotes for the ISFET threshold voltage. Considering power supplies of $\pm$ 5.0 V, a 0.5 MΩ for R_{DS} and a 1.0 μA for I_{BIAS1} were chosen to bias the ISFET in the linear region with a 0.5-V drop in its source-and-drain terminals. To draw a 1.0 μA of I_{BIAS1}, a R_4 of 4 MΩ with a V_{B1} of 1.0 V were used, since $I_{BIAS1} = (V_{CC} - V_{B1})/R_4$. On the other hand, a 4 μA of CC current was drawn by I_{BIAS2} which demanded a resistor R_2 of 1 MΩ and a V_{B2} of -1.0 V. Resistors R_1 and R_3 (both 10 kΩ) were used to ensure the BJTs operation in active-mode.

The output V_{out}, measured using a digital multimeter, ranged from -660 mV to -336 mV over the pH value of 4 to 7 and from -336 mV to -12 mV over the pH value of 7 to 10, indicating a -648 mV of span and a 108 mV/pH of responsivity over the pH 4 to 10. Additionally, a 1 of R^2 coefficient was found, denoting 100% of fit between frequency and pH over the linear regression model.

The aforementioned results between the source-drain follower and the proposed pHCO circuit are better found in the plot of Figure 12.

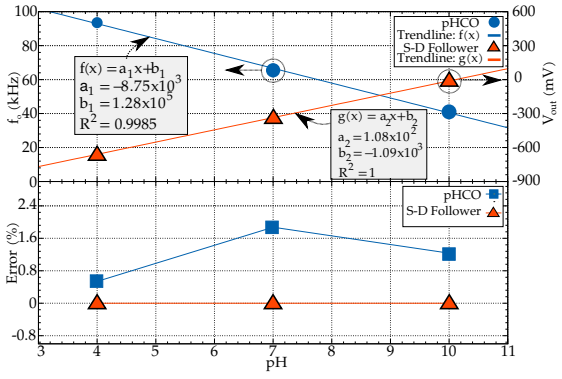

Fig. 12: The pHCO and the Source-Drain Followers discrete-circuit results and its respective linear trendlines

VI. Conclusion

This paper presented an AFE to condition the electrically-weak signal of an ISFET-based sensor directly to digital domain using a pulse frequency modulation technique. Both static and dynamic circuit operation were analyzed and the self-biasing configuration, based on a serie-series feedback loop, has been used to tie the ISFET DC operation point. Further, the circuit is insensitive to the body effect constraints and still suppress the use of AMP-OPs or ADCs - which contributes for complexity minimization and power saving of the instrumentation system. The sensor's parameters extraction have been used in the Verilog-based model for aiding electrochemical simulations and the conditioning technique was demonstrated from the electrochemical results of the discrete-circuit implementation. Oscilloscope measurements revealed digital waveforms in the output and the results using pH 4, pH 7 and pH 10 of buffer solutions found 0.9985 of R^2 coefficient and 2 % of uppermost linearity error, denoting its goodness of fit with the linear model. Moreover, it can be inferred from the results, in average, a 26 kHz of span over the pH 4 to 10 and a 9 kHz/pH of AFE responsitivity.

Acknowledgment

This work was partially supported by CNPq, INCT-NAMITEC and CAPES. We are thankful to the Centro de Componentes Semicondutores (CCS) from Unicamp, Brazil, for furnishing ISFETs samples.

References

[1] P. Bergveld, "Thirty years of ISFETOLOGY: What happened in the past 30 years and what may happen in the next 30 years," *Sensors and Actuators B: Chemical*, vol. 88, no. 1, pp. 1–20, 2003.

[2] B. Palán, F. V. Santos, J. M. Karam, B. Courtois, and M. Husák, "New ISFET sensor interface circuit for biomedical applications," *Sensors and Actuators B: Chemical*, vol. 57, no. 1–3, pp. 63–68, 1999.

[3] V. P. P. Chodavarapu, a. H. Titus, and a. N. Cartwright, "CMOS ISFET Microsystem for Biomedical Applications," *IEEE Sensors, 2005.*, vol. 41, no. 12, pp. 109–112, 2005.

[4] L. Bousse, N. De Rooij, and P. Bergveld, "Operation of chemically sensitive field-effect sensors as a function of the insulator-electrolyte interface," *IEEE Transactions on Electron Devices*, vol. 30, no. 10, pp. 1263–1270, oct 1983.

[5] S. Martinoia and G. Massobrio, "A behavioral macromodel of the ISFET in SPICE," *Sensors and Actuators B: Chemical*, vol. 62, no. 3, pp. 182–189, mar 2000.

[6] A. Morgenshtein, L. Sudakov-Boreysha, U. Dinnar, C. G. Jakobson, and Y. Nemirovsky, "CMOS readout circuitry for ISFET microsystems", *Sensors and Actuators B: Chemical*, vol. 97, no. 1, pp. 122–131, 2004.

[7] P. K. Chan and D. Y. Chen, "A CMOS ISFET Interface Circuit With Dynamic Current Temperature Compensation Technique," *Circuits and Systems I: Regular Papers, IEEE Transactions on*, vol. 54, no. 1, pp. 119–129, 2007.

[8] Y. Liu, a. Al-Ahdal, P. Georgiou, and C. Toumazou, "Minimal readout scheme for ISFET sensing arrays based on pulse width modulation," *Electronics Letters*, vol. 48, no. 10, p. 548, 2012.

[9] W. P. Chan, B. Premanode, and C. Toumazou, "An Integrated ISFETs Instrumentation System in Standard CMOS Technology," *IEEE Journal of Solid-State Circuits*, vol. 45, no. 9, pp. 1923–1934, sep 2010.

[10] J. van der Tang, D. Kasperkovitz, and A. H. van Roermund, "High-Frequency Oscillator Design for Integrated Transceivers", Kluwer Academic Publishers, ISBN=1402075642, 2006.